Imagined Head Rotations Facilitate Spatial Memory

Gerda Wyssen (gerda.wyssen@unibe.ch)
University of Bern
Fred W. Mast
University of Bern
Matthias Ertl
University of Bern

Research Article

Keywords: efference copy, corollary discharge, motor imagery, active motion, head kinematics, vestibular, motor execution

Posted Date: February 4th, 2022

DOI: https://doi.org/10.21203/rs.3.rs-1316811/v1

Abstract

Neuroimaging studies have shown great similarities between the cortical networks involved in motor execution and motor imagery. However, none of those studies report data on head or full body motions and only few provide evidence of behavioral consequences of this similarity. Here, we report results from a novel kinesthetic spatial memory task, in which participants encoded a target position by an active, passive or imagined head rotation. During the experiment, participants were seated on a motion platform with a VR headset, which allowed passive motion and head tracking. To compare all three encoding conditions, precision and head velocity in the executions of head movements were analyzed with Bayesian hierarchical generalized linear regression models. We found comparable performance in precision in the active and imagery conditions whereas performance in the passive condition was significantly reduced. Head motion profiles were similar after active and imagined encoding. The results suggest that imagined head rotations provide useful sensorimotor information despite the absence of sensory and motor information during encoding. This can be explained by corollary discharge which is necessary for appropriate motor behavior and is likely also generated when the motor behavior is imagined but not executed.

Introduction

The term spatial memory refers to stored information regarding the location of objects or the self in three-dimensional space. Spatial memory is a prerequisite for an efficient and goal directed interaction with the environment. It is relevant for spatial reasoning and learning, spatial updating, and successful navigation. Various sensory systems are involved in spatial memory such as the visual, auditory, somatosensory, vestibular and the proprioceptive system [1]. The integration of different sensory sources of information requires spatial and temporal transformations between modality specific reference frames [2], [3]. Despite the multisensory nature of spatial memory most research in the field relies on unimodal tasks in the visual domain (PC-based maze tasks). It is surprising that vestibular input has been widely disregarded despite compelling evidence for its important contribution in spatial memory [4]–[7]. Psychophysical experiments demonstrated that humans store information regarding translational and rotational movements in spatial memory [8]. They can reproduce the distance of a previously experienced passive movement, and its dynamic properties like the specific velocity profile of the perceived passive motion [9]. Moreover, clinical studies demonstrated that complete loss of vestibular function led to decreased performance in spatial memory [10]. Decreased function of the otolith organs, the part of the vestibular organ detecting translational accelerations, is associated with decreased hippocampal volume [10], [11], one of the central brain structures for spatial memory [12]. Further evidence for the importance of the vestibular input in spatial memory is provided by animal research. Nguyen and colleagues [13] investigated spatial memory in mice and compared the performance before and after a unilateral labyrinthectomy (surgical removal of the vestibular end organ). Performance in a Y-Maze and Morris Water Maze task was dramatically reduced after labyrinthectomy. Interestingly, galvanic vestibular stimulation accelerated the recovery of spatial memory performance after the labyrinthectomy. In

humans, stimulation of the vestibular system can lead to improved spatial memory performance. For example, Hilliard and colleagues [14] reported that galvanic vestibular stimulation improves performance in spatial memory when compared to sham stimulation in a virtual spatial navigation task. In summary, studies in animals and humans show that spatial memory is relying heavily on self-motion cues that involve vestibular information.

Self-motion cues contributing to spatial memory are not only perceived passively, but they are often the result of active motion. The distinction between active and passive motion is crucial for moving organisms, and it is provided by the efference copy of the motor command [15], [16] or corollary discharge [17]. While many authors use these terms interchangeably, others emphasize conceptual differences. Crapse and Sommer [18] pointed out that motor related signals can influence sensory processes on various stages along the processing chain and that the term efference copy implies that one is referring to an actual copy of the motor commands targeting the muscles. Following this definition, the term efference copy is tied to overt motor behavior. Motor to sensory signals occurring at higher levels are summarized under the more general term corollary discharge, including mental processes like motor imagery. We will use this distinction for the further description of the study.

Efference copies are used to predict the sensory consequences of one's own motor behavior. The predicted input allows to compensate the reafferent input and it can alter the sensory processing in the respective primary cortices. For example, the efference copy can explain why we cannot tickle ourselves. When we initiate the movement of tickling ourselves, we can simply anticipate the sensory tactile consequences whereas the exact same tactile stimulation executed by someone else cannot be precisely anticipated and elicits a strong tickling sensation. Attenuating the sensory processing of self-generated activation reduces redundant information, increases the signal-to-noise ratio, and therefore allows for a more efficient processing of sensory information. It is known that efference copy can increase performance in spatial memory tasks. For example, a study where target positions had to be encoded on a two-dimensional surface found a beneficial effect when encoding was combined with a hand and/or eye-movement towards the target compared to no movements [19], [20]. Moreover, studies investigating elbow [21] and hand-movements [20], [22] reported increased accuracies for conditions with active motor execution compared to no-motion. In addition to this, EEG studies on speech production successfully demonstrated that the auditory response to self-generated phonemes is reduced compared to passive listening [23].

Interestingly, these attenuation processes are still found when motor imagery is used to elicit a corollary discharge. For example, an attenuation of the auditory N1 amplitude can be observed when the imagined phoneme is paired with a matching playback [24]. In addition to efficient motor behavior, corollary discharges are, despite the absence of any overt motor action, also involved in simulation of motion such as imagined self-motion. Indeed, a recent study on motor imagery and touch suggested a functional equivalence between imagined and executed movements [25]. The authors stated that both processes engage the same sensory-motor mechanisms, including the generation of corollary discharge, the prediction of sensory consequences, and a specific attenuation of the sensory areas. Moreover, beneficial

effects of motor imagery have been demonstrated in motor neurorehabilitation. For example, motor imagery training of hand movements can be as effective as motor execution training in patients with hemiparesis [26] The emulation theory of mental representation suggests that motor execution, motor imagery and action observation rely – to a large extent – on the same neural infrastructure [27]. This is consistent with findings of meta-analyses of neuroimaging studies [28], [29] reporting similarities between the brain networks across these three processes. Surprisingly few studies have focused on spatial memory and corollary discharge in the domain of self-motion perception, and it therefore remains unclear whether findings observed for finger, arm, or leg motions transfer to head or full-body rotations. While corollary discharge is well studied in animals [18], [30], [31], a direct observation in humans remains challenging.

In our study, we investigated the relationship of active, passive, and imagined head rotations with positioning errors in a novel kinesthetic spatial memory task to isolate the effects of efference copy, corollary discharge, and self-motion cues. Participants encoded a target position under three conditions and we then compared motor execution of head movements to the encoded target position. Based on the results of previous studies, we expected a better performance when movements are actively executed compared to passive self-motion. With respect to the motor imagery condition two lines of argumentation are plausible. First, it is possible that motor imagery will lead to poor performance because neither sensory nor motor information is available during encoding. However, if the emulation theory of representation is correct, the brain simulates the consequences of the imagined action and therefore compensates the lack of sensorimotor interaction.

Methods

Participants

The required sample size for this experiment was calculated based on a medium effect size d = 0.4, an alpha-level of 0.05, and a power of 0.8. This resulted in a sample size of N = 52 participants for the comparison between the active and passive condition. In total 55 participants (39 females, 16 males, mean age: 22.4 years, SD: 3.4 years) were recruited through the student pool of the Institute of Psychology and received course credits for compensation. According to the 10 items handedness questionnaire [32], 45 participants were right-handed, 6 were left-handed and 3 were ambidextrous. The study was carried out in accordance with the Declaration of Helsinki and ethical approval was obtained from the Ethics Committee of the University of Bern.

Apparatus

For the experiment participants were seated in a racing chair mounted on a six degree of freedom motion platform (Fig. 1, panel **a**; 6DOF2000E, MOOG Inc., East Aurora NY). All motions performed by the platform were single cycle sinusoidal acceleration motion profiles with a peak velocity of 8.6°/s about the yaw axis. Throughout the entire experiment participants wore a head mounted virtual-reality headset (HTC Vive). A one-word instruction ("active", "passive", "imagine") was presented via speakers previous to each

trial. Button presses were registered by a game-controller. All mentioned components were controlled by PlatformCommander, an open-source software for interfacing motion platforms [33], [34].

Stimuli

During the experiment visual stimuli were presented via a head mounted display. The stimuli were generated by PlatformCommander using the OpenGL environment (https://www.opengl.org/). Unless during the retrieval phase, a green sphere indicating the straight-ahead position of the participant was visible. The sphere was modeled with a diameter of 5.0 centimeters. The position of the sphere was adjusted according to the participants head movement based on the sensor data provided by the VR goggles. The world-fixed center of the scene was visualized by a red sphere of 4.5 centimeter diameter and the target by a yellow sphere with a diameter of 5.5 centimeter. All spheres were presented at a virtual distance of 1.5 meter. At the beginning of each trial a fixation cross with an arm length of 40 centimeters was presented at the same distance.

Procedure

After participants gave their written consent, they were seated on the motion platform. The participant's handedness was orally inquired by the ten-item Edinburgh inventory [32]. We accounted for individual differences in interpupillary distance with lens adjustments to enable 3D vision and to avoid diplopia. In order to calibrate the world-fixed center, participants were asked to relax and position their head in a natural straight-ahead position. The center position was re-calibrated after seven trials throughout the experiment to compensate the drift rate of the gyroscope. The experiment consisted of 4 blocks with 48 trials each. During each block 14 target positions (±3, ±6, ±9, ±12, ±15, ±18, ±21) were tested for all three conditions. Targets were presented in the horizontal (yaw) plane to the left and right of the center. Throughout this manuscript negative angles refer to targets located to the left of the center. The order of the trials was randomized for each block and participant. Prior to the experiment six training trials (two per condition) allowed the participants to get familiar with the task, to experience the passive motion and to ask questions. Between the blocks, participants performed guided head movements for 60 seconds to relax their neck muscles.

Each trial (Fig. 1, panel **b**) started with a single word auditory instruction ("active", "passive", "imagine") followed by a fixation cross appearing on the screen. The color of the cross also indicated the type of the trial (green = active, red = passive, blue = imagery). The fixation cross was presented at the center of the virtual room (straight-ahead) and to start a trial the participants had to position their head direction (naso-occipital axis) at the center of the cross. The encoding phase started once the participant aimed their head direction at the center for one second the cross disappeared, and the target (yellow sphere) was presented at one of the target positions. In the active condition, participants were asked to rotate their head to the target. After the head position matched the target by less than one centimeter for one second, the target disappeared, and the participants returned their head direction to the center. In the passive condition, the participants were instructed not to make voluntary head movements. The motion platform rotated the participant to the target position, remained there for one second, and returned to the center. In

the imagery condition, participants were asked to imagine a head movement to the target without moving their head or eyes. The appearance and disappearance of the visual cues followed the exact pattern as in the passive condition. In all three conditions, participants had to position their head direction at the center for one second with an accuracy of less than one centimeter before all visual cues disappeared. In the recall phase, participants were then instructed to rotate their head to the encoded target position and confirm the position via button press. A video showing an example trial of each condition is available online (https://tube.switch.ch/videos/wYJPDMbzPj#29). The acceleration data provided by the VR headset were logged by PlatformCommander at 1000 samples per second and later exported with a rate of 20 samples per second.

At the end of the experiment, participants were asked to rate the vividness of their motor imagery experience during the imagery trials on a 10-point Likert scale, where 0 indicated a poor and 10 an excellent imagery quality.

Data analysis

Data analysis was conducted in R [35] using Rstudio [36] and the packages 'brms' [37], 'tidybayes' [38], and 'tidyverse' [39] if not mentioned otherwise. Plots were created with Matlab (2019b, Mathworks). If not otherwise mentioned, we weakly informative default priors were chosen for Bayesian hierarchical generalized linear regression after checking them for plausibility based on physiological head movements. To ensure that the chosen priors did not influence the results of the analysis, the analyses were also run with less and more informative priors. All models were run with 4 chains and 6000 iterations, and delta and tree depth values were increased when R-hat values were above 1.01. To be sure the model fitted the data well, pareto-k diagnostics were checked for values above 0.5 and posterior predictive plots were visually inspected. To quantify the variance explained by the model the Bayesian R2 value for the model was calculated [40]. If the 95% credible interval of the posterior distribution of the estimated beta weights did not contain zero, a meaningful difference of the parameter from zero was inferred. Model equations including prior specifications and checks for model fits are described in the supplementary materials (Supplementary S1).

Position Data

For the main analysis, absolute errors were taken as a measure for the precision of the angle estimation during the recall. Absolute errors were calculated as difference between the head position in the recall and the target angle, irrespective of the direction of the error. In order to test if there are meaningful differences in absolute errors between the three conditions (active, passive, imagery), we used a Bayesian hierarchical generalized linear regression model with the active condition as intercept. Random intercepts for every participant and absolute target position were included to account for individual accuracy and the influence of target positions on the errors. Absolute target positions were included as factors, because of a non-monotonic influence on the absolute errors. As the absolute errors are not normally distributed but rather left-shifted, a log-normal link-function was used. Additionally, we fitted a model with imagery

scores as population-level effect and random intercepts for every participant and absolute target position to check if self-rated vividness influenced performance in the imagery condition.

To analyze the direction of the errors, we visually inspected the error patterns over all participants, as well as for every single participant. For quantification, we fitted a Bayesian hierarchical generalized linear regression model with a gaussian link-function to estimate the effect of condition (active, passive, imagery) and the absolute target position, as well as the interaction thereof on errors. Random intercepts and slopes for condition and target position and interactions were also included for every participant.

Motion Profiles

The position information obtained by the VR-headset was imported to Matlab (2019b, Mathworks) at a sampling rate of 20 samples per second. The velocity profiles were calculated using the difference between two data points as an estimate for the first derivative. Because it is difficult to detect the exact motion onset of the head rotation all trials were aligned based on their peak velocities and segmented from -200 to 200 ms relative to this point. After visual inspection, data of four participants were excluded from this analysis because of issues in logging the data (2 participants), or because their head rotations did not consist of a smooth trajectory with a clear peak in more than 10% of the trials (2 participants). For the analysis all trials per participant were averaged, relative to the peak velocity, for each of the target angles. To compare absolute peak velocities in the recall phase a Bayesian hierarchical generalized linear regression model with a gaussian link-function was used to estimate the influence of the condition (active, passive, imagery) and the absolute target position, as well as the interaction of both. Random intercepts and slopes for condition and absolute target angle and interaction thereof were also included for every participant. For the intercept of absolute peak velocities, a uniform prior between 0 and 200 deg/s and for the beta weights a student-t distribution with a mean of 0, a standard deviation of 50 and 3 degrees of freedom were chosen.

Results

Position Data

All participants completed the experiment. One data set has been removed from the analysis because the participant rotated their head only by about 1.3° (SD = 1.85°) across all trials during retrieval, which indicates that the participant did not perform the task as instructed.

The positioning error of the head movement to the required target, i.e. median of absolute error, was 1.95° (range: 1.21° - 9.86°) over all participants and conditions. Absolute errors were smallest in the active condition (median: 1.83°, range: 0.75° - 9.65°) and largest for the passive condition (median: 2.34°, range: 1.18° - 9.82°). The absolute median error for the imagery condition was 1.87° (range: 1.23° - 10.14°) and therefore close to the absolute error in the active condition (Fig. 2). In the Bayesian regression model, the active condition was the intercept ($\beta_{\text{intercept}}$ = 0.42, 95% CI [0.14, 0.71]). Compared to this intercept, the imagery condition did not change the performance in the task ($\beta_{\text{imagery condition}}$ = 0.00, 95% CI [-0.05,

0.06]). However, the passive condition ($\beta_{\text{passive condition}}$ = 0.26, 95% CI [0.20, 0.31]) led to worse performance than both the active and the imagery condition. Estimates are reported on the log-scale. Therefore, estimates for imagery and passive condition indicate percentage of change in task performance with respect to the active condition.

The Bayesian R2 value, 0.36, 95% CI [0.32, 0.39], suggests that the model accounted for approximately 36% of the variance in the data. Overall, we found better performance in the active and imagery condition when compared to the passive condition, indicating a beneficial effect of motor imagery on performance in the spatial memory task. This effect is illustrated in Fig. 2. Self-rated vividness did not show meaningful influence on absolute errors in the imagery condition. Data of one additional participant had to be excluded from this analysis because of missing values.

To further investigate the effect of the condition on errors, we compared the raw error patterns in all conditions and target angles. In the active condition all target angles were overestimated (participants turned their heads too far). In the passive condition target angles between 3° and 12° were overestimated and angles larger than 18° were systematically underestimated. A similar pattern was found in the imagery condition. However, the transition between over- and underestimation occurred between 9° and 12°. Upon visual inspection, most of the participants showed an error pattern comparable to the pattern reported above with overestimation in the active condition and reversing errors in the passive and imagery conditions.

In the Bayesian regression model, the active condition was the intercept ($\beta_{\text{intercept}}$ = 1.79, 95% CI [1.44, 2.14]), showing an overestimation in the active condition. As in the model with absolute errors, the imagery condition overall led to comparable errors ($\beta_{\text{imagery condition}}$ = 0.03, 95% CI [-0.29, 0.35]), but passive condition ($\beta_{\text{passive condition}}$ = 1.31, 95% CI [1.00, 1.61]) overall led to smaller errors compared to the intercept. Errors did not vary with respect to target angles ($\beta_{\text{target angle}}$ = -0.02, 95% CI [-0.06, 0.00]), reflecting a constant overestimation in the active condition. However, an interaction of target angle with the imagery condition ($\beta_{\text{imagery condition * target angle}}$ = -0.13, 95% CI [-0.16, -0.10]), and to a larger extent with the passive condition ($\beta_{\text{passive condition * target angle}}$ = -0.16, 95% CI [-0.63, -0.46]) was found, showing that in smaller target angles errors were due to overestimation but changed to underestimation errors with increasing angles. Estimates are reported in degrees. The Bayesian R2 value, 0.46, 95% CI [0.44, 0.47], suggests that the model accounted for approximately 46% of the variance in the data.

Motion profiles

We also analyzed the kinematics of the active head rotation during the retrieval. The grand averages across all participants for each condition and target angle are visualized in Fig. 3. We found that the head rotations showed a reliable sinusoidal shaped acceleration pattern similar to the passive stimuli used in most perception studies. In all conditions, the peak velocity increased for larger target angles. An interesting pattern was observed for the passive, compared to the active and imagery condition. The peak

velocities showed a reduced range with larger peak velocities for small angles but smaller peak velocities for large target angles (Table 1 & Fig. 3, panel **g** & **h**). In the Bayesian model with active condition as intercept ($\beta_{\text{intercept}}$ = 9.64, 95% CI [8.43, 10.80]), this is reflected in a larger velocity of the passive condition in the smallest target angle ($\beta_{\text{passive condition}}$ = 6.08, 95% CI [5.27, 6.92]) but no difference in the imagery condition ($\beta_{\text{imagery condition}}$ = 0.59, 95% CI [-0.19, 1.36]). Additionally, an interaction of target angle with the passive condition ($\beta_{\text{passive condition * target angle}}$ = -0.55, 95% CI [-0.63, -0.46]), and to a smaller extent with the imagery condition ($\beta_{\text{imagery condition * target angle}}$ = -0.20, 95% CI [-0.27, -0.13]) was found, showing less spread in these conditions, much stronger pronounced in the passive condition. Overall peak velocity increased with larger target angles ($\beta_{\text{target angle}}$ = 1.07, 95% CI [0.96, 1.18]). The Bayesian R2 value, 0.67, 95% CI [0.67, 0.68], suggests that the model accounted for approximately 67% of the variance in the data.

Table 1
Median peak velocities of the head rotation during the retrieval per target angles and condition. The spread of head velocity among the different target angles is calculated by subtracting the minimal from the maximal peak velocity.

	3°	6°	9°	12°	15°	18°	21°	spread
active	7.2	10.7	12.8	15.3	18.2	19.9	20.8	13.6
passive	10.9	12.0	14.1	15.1	15.8	16.3	16.7	5.8
imagery	7.3	10.9	12.6	14.1	15.9	15.0	19.5	12.2

Discussion

We investigated spatial memory using a novel kinesthetic spatial memory task on a motion platform. We found that the encoding of a head rotation by an actively executed and an imagined head rotation leads to smaller errors when moving the head to the memorized position compared to an encoding by means of a passive rotation. The observation of a better performance in the active compared to the passive condition is unsurprising, as in the active condition encoding and retrieval are implemented by the same sensorimotor processes. In the passive condition, no motor commands are prepared and conveyed to the muscles, hence no efference copy is generated, and vestibular information is the only information related to self-motion. An essential component of our study design was the inclusion of a motor imagery condition, which was not part of previous studies. We have found that imagining a head rotation, without performing it during encoding, leads to similar performance as an actively performed head rotation and to better performance compared to the passive condition. No supportive sensory input was available during imagery while in the passive condition the vestibular, and in the active condition all information related to the head motion was available.

It has been theorized that during imagery sensory information is simulated internally by means of corollary discharge [41], [42]. Our study provides first empirical evidence of a specific influence of corollary discharge on spatial memory. Indeed, the emulation theory of mental representation proposes

that corollary discharge inform the same forward-models activated by the motor signals during active motions and therefore induce a full emulation of the expected sensory perceptions [27]. Recent findings in the tactile domain demonstrated that imagined self-touch is attenuated just as real self-touch [25]. The emulation of the motor signals and the sensory consequences might also be the explanation for the good performance of the participants in the imagery condition in our study.

We found differences in the error patterns for the increasing target angles between the three conditions. In the active condition, the targets were consistently overestimated across all angles (Fig. 2, panel **b**). This is in line with results obtained by studies using a cervical joint positioning task [43]–[45], where healthy controls tend to overshoot the target position after an active head rotation. Similar overshoots are known from experiments investigating shoulder movements [46]. Interestingly, encoding via an imagined rotation resulted in a more complex error pattern. A pronounced overestimation was only observed for the small target angles between 3° and 9°, while the retrieval position for the angles of 12° and 15° were even more accurate than in the active condition (Fig. 2, panel **d**). For the large angles (18° and 21°) the targets were underestimated. A similar pattern was found for the errors in the passive condition. However, the overestimation of the small target angles was more pronounced than in the imagery condition (Fig. 2, panel **c**). The similarity of error patterns in the imagery and passive condition could suggest that the participants imagined passive rather than active rotations. In the future, this could be tested by explicitly instructing the participants to imagine either a passive or an active head rotation and by comparing the error-patterns resulting from the manipulation. However, the head velocity patterns do not support the above explanation, because head velocity patterns in the imagery condition were comparable to the patterns in active condition. Head velocity in the passive condition, however, more restricted shown in less variation of head velocity between the minimal and maximal target angle (Table 1 and Fig. 3, panel **g** & **h** embedded in panel **a**)). The most plausible explanation for the smaller variance in peak accelerations in passive condition is that the participants incorporated the velocity properties into their head rotations. Due to the technical limitations of the motion platform, it is impossible to match the peak velocities occurring during active head rotations for large target angles. For this reason, rotation profiles with the same peak velocity were used for all target angles in the passive condition while in active and imagery condition head velocities were individual and not restricted. Overall, the analysis of the movement profiles showed that the movement type during encoding influenced the peak velocities of motor execution during retrieval. This finding confirms previous reports [9] on the impact of passively experienced motion profiles on subsequent attempts to actively replicate the motion profiles.

The current study raises interesting questions that could be addressed in future studies. For example, it is unclear whether the decreased performance in the passive compared to the active condition is due to the lack of proprioceptive (neck-muscle) information. This question could be addressed by adding a condition where the head is actively rotated by the participant, while the platform performs a counter rotation. By doing so, the head would rotate on the trunk without perceiving acceleration via vestibular receptors but still generating an efference copy and muscle activity. In this experiment, we were unable to test angles larger than 21° because of the restrictions of the motion platform, but it would be interesting to explore if the underestimation in imagery and passive condition keeps increasing (Fig. 2, panel **c** & **d**)

for angles beyond 21° or if a plateau is reached at some point. Moreover, the vividness of motor imagery as assessed by a single question did not predict performance in the imagery condition. Future studies could use more detailed questionnaires to assess individual imagery ability, as well as vividness ratings after each imagery trial to account for response tendencies of the participants and varying imagery strength from trial to trial.

Taken together, we provided first evidence for the impact of motor imagery on spatial memory performance. The kinesthetic spatial memory task is suitable to investigate the similarities and differences between active, passive and imagined motion during encoding. The results demonstrate the beneficial capabilities of motor imagery in a multi-sensory, non-visual task, and they strengthen the role of corollary discharge in cognitive tasks. This research is also relevant for cognitive and sports scientists, as well as clinicians, who aspire to develop imagery training, for example to promote brain recovery after stroke, or to boost performance in athletes.

Declarations

Acknowledgment

We thank Lea Saric, Yasmine Bühlmann, and Andreas Szukics for their help in the data acquisition process and Lilla Gurtner and Andrew Ellis for valuable comments on the manuscript. We are also grateful for the support of the Technology Platform of the Human Sciences Faculty.

Authors contributions

M.E. designed and conducted the experiment. M.E. and G.W. prepared and analyzed the data. M.E., G.W. and F.M. wrote the manuscript.

Data availability

Data and code is available in the supplementary materials (Supplementary Dataset). Identifying details such as age, gender and handedness have been removed.

Additional information

The authors declare no competing interests.

References

1. Herweg, N. A. & Kahana, M. J. Spatial Representations in the Human Brain. *Front. Hum. Neurosci.* **12**, (2018).
2. Chen, X., DeAngelis, G. C. & Angelaki, D. E. Diverse spatial reference frames of vestibular signals in parietal cortex. *Neuron* **80**, 1310–1321 (2013).

3. Burgess, N. Spatial memory: how egocentric and allocentric combine. *Trends Cogn. Sci.* **10**, 551–557 (2006).
4. Mast, F. W., Preuss, N., Hartmann, M. & Grabherr, L. Spatial cognition, body representation and affective processes: the role of vestibular information beyond ocular reflexes and control of posture. *Front. Integr. Neurosci.* **8**, 1–14 (2014).
5. Brandt, T., Strupp, M. & Dieterich, M. Towards a concept of disorders of “higher vestibular function”. *Frontiers Integr. Neurosci.* **8**, 1–8 (2014).
6. Brandt, T., Zwergal, A. & Glasauer, S. 3-D spatial memory and navigation: Functions and disorders. *Curr. Opin. Neurol.* **30**, 90–97 (2017).
7. Smith, P. F. The Growing Evidence for the Importance of the Otoliths in Spatial Memory. *Front. Neural Circuit.* **13**, (2019).
8. Israel, I., Chapuis, N., Glasauer, S., Charade, O. & Berthoz, A. Estimation of passive horizontal linear whole-body displacement in humans. *J. Neurophysiol.* **70**, 1270–1273 (1993).
9. Berthoz, A., Israel, I., Georges-Francois, P., Grasso, R. & Tsuzuku, T. Spatial memory of body linear displacement: what is being stored? *Science* **269**, 95–98 (1995).
10. Brandt, T. *et al.* Vestibular loss causes hippocampal atrophy and impaired spatial memory in humans. *Brain* **128**, 2732–2741 (2005).
11. Kamil, R. J., Jacob, A., Ratnanather, J. T., Resnick, S. M. & Agrawal, Y. Vestibular Function and Hippocampal Volume in the Baltimore Longitudinal Study of Aging (BLSA). *Otol. Neurotol.* **39**, 765–771 (2018).
12. Eichenbaum, H. The role of the hippocampus in navigation is memory. *J. Neurophysiol* **117**, 1785–1796 (2017).
13. Nguyen, T. T. *et al.* Galvanic Vestibular Stimulation Improves Spatial Cognition After Unilateral Labyrinthectomy in Mice. *Front. Neurol.* **12**, 716795 (2021).
14. Hilliard, D. *et al.* Noisy galvanic vestibular stimulation modulates spatial memory in young healthy adults. *Sci. Rep.* **9**, 1–11 (2019).
15. von Holst, V. E. & Mittelstaedt, H. Das Reafferenzprinzip (Wechselwirkungen zwischen Zentralnervensystem und Peripherie). *Die Naturwissenschaften* **20**, (1950).
16. Cullen, K. E. Sensory signals during active versus passive movement. *Curr. Opin. Neurobiol.* **14**, 698–706 (2004).
17. Sperry, R. W. Neural basis of the spontaneous optokinetic response produced by visual inversion. *J. Comp. Physiol. Psychol.* **43**, 482–489 (1950).
18. Crapse, Trinity B & Sommer, M. A. Corollary discharge across the animal kingdom. *Nat. Rev. Neurosci.* **9**, (2008).
19. Burke, M. R., Clarke, J. B. & Hedley, J. Effect of retinal and/or extra-retinal information on age in memory-guided saccades. *Exp. Brain Res.* **205**, 87–94 (2010).

20. Gonzalez, C. C. & Burke, M. R. The brain uses efference copy information to optimise spatial memory. *Exp. Brain Res.* **224**, 189–197 (2013).
21. Gritsenko, V., Krouchev, N. I. & Kalaska, J. F. Afferent Input, Efference Copy, Signal Noise, and Biases in Perception of Joint Angle During Active Versus Passive Elbow Movements. *J. Neurophysiol.* **98**, 1140–1154 (2007).
22. Adamovich, S. V., Berkinblit, M. B., Fookson, O. & Poizner, H. Pointing in 3D Space to Remembered Targets. I. Kinesthetic Versus Visual Target Presentation. *J. Neurophysiol.* **79**, 2833–2846 (1998).
23. Oestreich, L. K. L. *et al.* Subnormal sensory attenuation to self-generated speech in schizotypy: Electrophysiological evidence for a 'continuum of psychosis'. *Int. J. Psychophysiol.* **97**, 131–138 (2015).
24. Whitford, T. J. *et al.* Neurophysiological evidence of efference copies to inner speech. *eLife* **6**, e28197 (2017).
25. Kilteni, K., Andersson, B. J., Houborg, C. & Ehrsson, H. H. Motor imagery involves predicting the sensory consequences of the imagined movement. *Nat. Commun.* **9**, 1617 (2018).
26. Grabherr, L., Jola, C., Berra, G., Theiler, R. & Mast, F. W. Motor imagery training improves precision of an upper limb movement in patients with hemiparesis. *NeuroRehabilitation* (2015).
27. Grush, R. The emulation theory of representation: Motor control, imagery, and perception. *Behav. Brain Sci.* **27**, 377–396 (2004).
28. Hétu, S. *et al.* The neural network of motor imagery: An ALE meta-analysis. *Neurosci. Biobehav. R.* **37**, 930–949 (2013).
29. Hardwick, R. M., Caspers, S., Eickhoff, S. B. & Swinnen, S. P. Neural correlates of action: Comparing meta-analyses of imagery, observation, and execution. *Neurosci. Biobehav. R.* **94**, 31–44 (2018).
30. Poulet, J. F. A. Corollary discharge inhibition and audition in the stridulating cricket. *J. Comp. Physiol. A* **191**, 979–986 (2005).
31. Cavanaugh, J., Berman, R. A., Joiner, W. M. & Wurtz, R. H. Saccadic Corollary Discharge Underlies Stable Visual Perception. *J. Neurosci.* **36**, 31–42 (2016).
32. Oldfield, R. C. The assessment and analysis of handedness: The Edinburgh inventory. *Neuropsychologia* **9**, 97–113 (1971).
33. Ertl, M., Prelz, C., Fitze, D. C., Wyssen, G. & Mast, F. W. PlatformCommander — An open source software for an easy integration of motion platforms in research laboratories. *SoftwareX* **17**, 100945 (2022).
34. Ertl, M., Prelz, C., Fitze, D. C., Wyssen, G. & Mast, F. W. Manual PlatformCommander Version 0.9. (2021) doi:10.5281/zenodo.5743201.
35. R-Core-Team. R: A Language and Environment for Statistical Computing. (2018).
36. RStudio-Team. RStudio: Integrated Development Environment for R. (2020).
37. Bürkner, P.-C. brms: An R Package for Bayesian Multilevel Models Using Stan. *Journal of Statistical Software* **80**, 1–28 (2017).

38. Kay, M. tidybayes: Tidy Data and Geoms for Bayesian Models. (2020).
39. Wickham, H. tidyverse: Easily Install and Load the Tidyverse. (2021).
40. Gelman, A., Goodrich, B., Gabry, J. & Vehtari, A. R-squared for Bayesian Regression Models. *The American Statistician* **73**, 307–309 (2019).
41. Subramanian, D., Alers, A. & Sommer, M. A. Corollary Discharge for Action and Cognition. *Biological Psychiatry: Cognitive Neuroscience and Neuroimaging* 1–9 (2019) doi:10.1016/j.bpsc.2019.05.010.
42. Tian, X. & Poeppel, D. Mental imagery of speech: linking motor and perceptual systems through internal simulation and estimation. *Front. Hum. Neurosci.* **6**, (2012).
43. M Revel, M., Andre-Deshays, A. & Minguet, M. Cervicocephalic Kinesthetic Sensibility in Patients with Cervical Pain. *Arch. Phys. Med. Rehabil.* (1991).
44. Heikkilä, H. V. & Wenngren, B. I. Cervicocephalic kinesthetic sensibility, active range of cervical motion, and oculomotor function in patients with whiplash injury. *Arch. Phys. Med. Rehabil.* **79**, 1089–1094 (1998).
45. Treleaven, J., Jull, G. & Sterling, M. Dizziness and unsteadiness following wiplash injury: Characteristic features and relationship with cervical joint position error. *J. Rehabil. Med.* 36–43 (2003) doi:10.1080/16501970306109.
46. Brindle, T. J., Nitz, A. J., Uhl, T. L., Kifer, E. & Shapiro, R. Measures of accuracy for active shoulder movements at 3 different speeds with kinesthetic and visual feedback. *J. Orthop. Sports Phys. Ther.* **34**, 468–478 (2004).

Figures

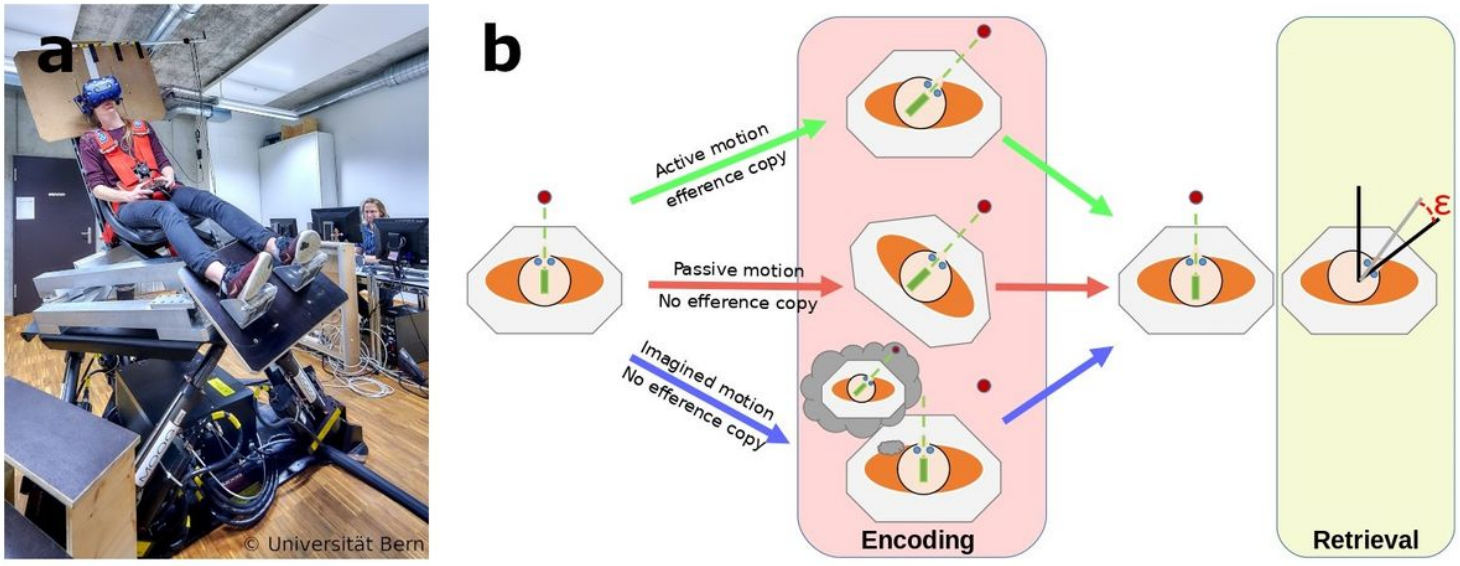

Figure 1

Experimental conditions

a) Picture of the motion platform used for the experiment. b) Visualization of the three conditions (encoding phase). In the active motion condition participants were asked to rotate their head in order to align it with a visual target and then return to the center. In the passive motion condition, the platform rotated the participants so that their naso-occipital axis pointed to the target before returning to the center. In the imagery condition participants were asked to imagine a head rotation towards the target and back as vivid as possible but without moving their head. In all conditions the visual cue disappeared once the participant returned to the center. Then, the participants were asked to rotate their head to the location where the target was presented during the encoding phase and confirm the position via button press (retrieval phase).

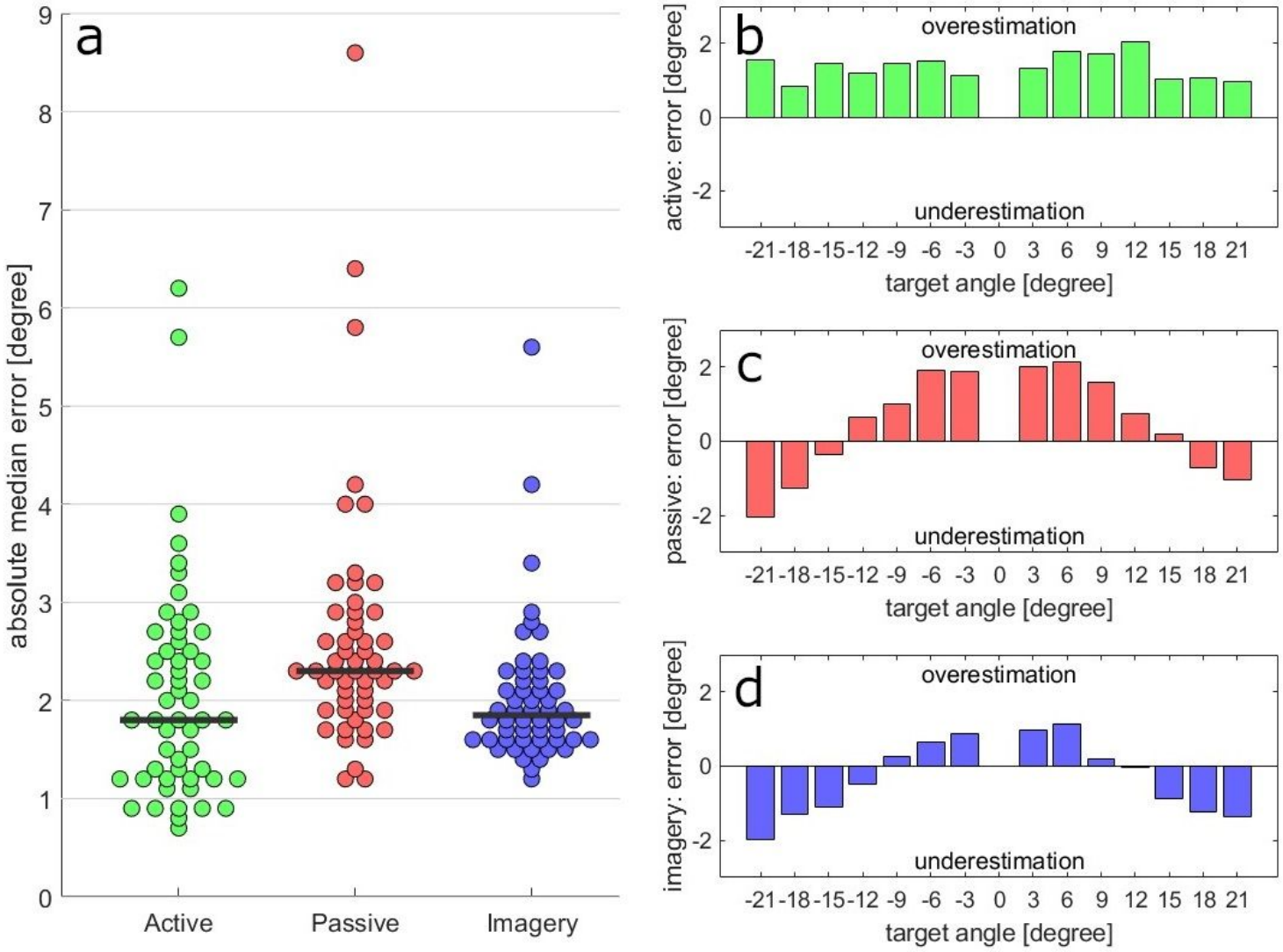

Figure 2

Absolute and raw errors of head rotations during recall

a) Visualization of the absolute errors per condition. Each dot represents the average error of one participant. The black bars indicate the median. b) Errors per target angles. In the *active* condition all target angles are overestimated by the participants. c) In the *passive* condition small target angles

(3°-12°) are over estimated, while larger angles (18° and 21°) were underestimated by the participants. d) The *imagery* condition shows a similar pattern as the *passive* condition. Small angles (3°-9°) are overestimated and larger target angles (12°-21°) are underestimated.

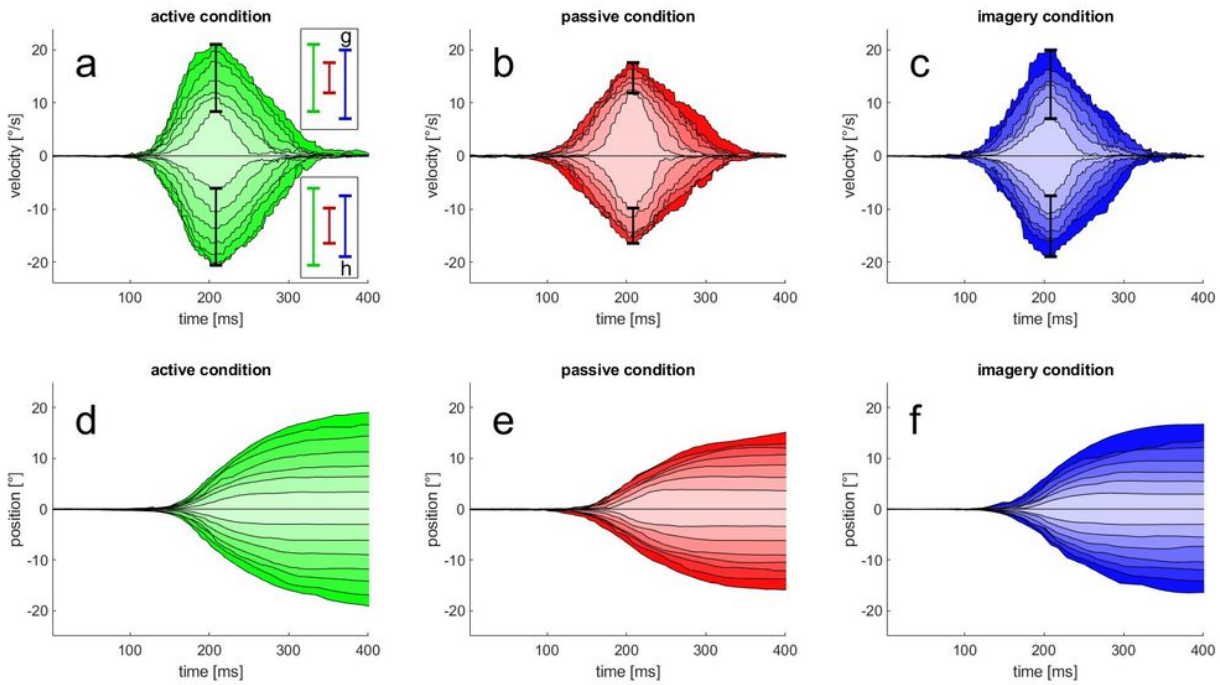

Figure 3

Head velocity and head position during recall

Visualization of the head velocity (a-c) and the head position (d-f) over time. The velocity profile is similar across all conditions and for all target angles. However, the peak velocity scales with the size of the target angle. Panel g and h, embedded in panel a, visualize the peak velocity spreads for each of the three conditions for clock and counterclockwise rotations. Surprisingly, the difference between the peak-velocity for the 21° target and the 3° target is smaller for the *passive* than for both other conditions.

Supplementary Files

This is a list of supplementary files associated with this preprint. Click to download.

- SupplementaryDataset.xlsx
- SupplementaryS1.pdf